JOURNAL OF Evolutionary Biology

doi: 10.1111/jeb.12985

Hot spots become cold spots: coevolution in variable temperature environments

A. B. DUNCAN*, E. DUSI*†, F. JACOB*, J. RAMSAYER*‡, M. E. HOCHBERG*§ & O. KALTZ*

*Institut des Sciences de l'Evolution, UMR 5554 (CC065), Université de Montpellier, Montpellier, France
†Institute for Hydrobiology, Technische Universität Dresden, Dresden, Germany
‡INRA, UMR 0320 Quantitative Genetics and Evolution, Gif-sur-Yvette, France
§Santa Fe Institute, Santa Fe, NM, USA

Keywords:

coevolution;
experimental evolution;
host–parasite;
microcosm;
phage;
Pseudomonas fluorescens;
temperature fluctuations.

Abstract

Antagonistic coevolution between hosts and parasites is a key process in the genesis and maintenance of biological diversity. Whereas coevolutionary dynamics show distinct patterns under favourable environmental conditions, the effects of more realistic, variable conditions are largely unknown. We investigated the impact of a fluctuating environment on antagonistic coevolution in experimental microcosms of *Pseudomonas fluorescens* SBW25 and lytic phage SBWΦ2. High-frequency temperature fluctuations caused no deviations from typical coevolutionary arms race dynamics. However, coevolution was stalled during periods of high temperature under intermediate- and low-frequency fluctuations, generating temporary coevolutionary cold spots. Temperature variation affected population density, providing evidence that eco-evolutionary feedbacks act through variable bacteria–phage encounter rates. Our study shows that environmental fluctuations can drive antagonistic species interactions into and out of coevolutionary cold and hot spots. Whether coevolution persists or stalls depends on the frequency of change and the environmental optima of both interacting players.

Introduction

Antagonistic coevolution between species, the reciprocal evolution of exploiter attack and victim resistance, is considered a major determinant of biodiversity and life history (Thompson, 2005, 2009). However, the factors driving the intensity of these interactions are still largely unknown. One idea is that the strength of the interaction varies in space and time, giving rise to coevolutionary hot and cold spots (Gomulkiewicz *et al.*, 2000). Coevolutionary hot spots typically describe regions of space, where interspecific interactions are strong and reciprocal, whereas in cold spots population interactions are asymmetric or nonexistent (Gomulkiewicz *et al.*, 2000; Nuismer *et al.*, 2003; Gibert *et al.*, 2013). Similarly, coevolutionary hot and cold spots may be present in time (Thompson, 2005).

Environmental variation may be an underlying cause of coevolutionary hot and cold spots (Lopez-Pascua & Buckling, 2008; Vogwill *et al.*, 2009). Abiotic conditions can directly affect the physiology of antagonist traits involved in infection or resistance, and thus whether the enemy can exploit its victim (and the victim defend itself) and/or the evolutionary potential of populations (genetic variation upon which selection can act, costs of resistance/infectivity). Indeed, theoretical work shows that the intensity of coevolution may vary across productivity gradients impacting victim demography, and thereby the force of infection (Hochberg & van Baalen 1998), an idea supported by experimental studies (Lopez-Pascua & Buckling, 2008; Harrison *et al.*, 2013). Thus, by modifying the potential for attack and defence, the environment can determine whether coevolution occurs (Thrall *et al.*, 2007; Wolinska & King, 2009), and the coevolutionary pattern observed (e.g. arms race vs. fluctuating selection dynamics) (Gómez & Buckling, 2011; Friman & Buckling, 2013).

Correspondence: Alison Duncan, Institute of Evolutionary Sciences, UMR 5554 (CC065), University of Montpellier, Place E. Bataillon, 34095 Montpellier Cedex 05, France.
Tel.: +33 (0)4 67 14 40 63; fax: +33 (0)4 67 14 40 61;
e-mail: Alison.duncan@umontpellier.fr

Experimental studies on the role of the environment in antagonistic coevolution have mostly focussed on spatial heterogeneity (Brockhurst *et al.*, 2003; Forde *et al.*, 2004; Lopez-Pascua & Buckling, 2008; Vogwill *et al.*, 2009; Lopez-Pascua *et al.*, 2010; Gorter *et al.*, 2016). Coevolution is more intense, with faster increases in resistance and infectivity, under high-resource (Lopez-Pascua & Buckling, 2008) and homogeneous conditions (Brockhurst *et al.*, 2003), possibly because encounter rates between players are higher (Brockhurst *et al.*, 2003; Lopez-Pascua & Buckling, 2008). Similarly, high-productivity environments promote patterns of parasite local adaptation (Forde *et al.*, 2004). These examples illustrate spatial coevolutionary hot spots.

Temporal environmental variation is predicted to influence coevolution differently from spatial variation (Nuismer *et al.*, 2003), but we are still lacking a good understanding of how common parameters, such as the amplitude or frequency of environmental fluctuations, affect coevolutionary hot and cold spots. A theoretical model by Poisot *et al.* (2011) predicts more intense coevolution for intermediate periods of high-resource conditions, equivalent to temporal 'hot spots'. Another model by Mostowy & Engelstädter (2011) shows that coevolutionary dynamics under low-frequency environmental fluctuations converge on dynamics observed in constant environments. Consistent with this prediction, Harrison *et al.* (2013) demonstrated that bacteria–phage coevolution was maintained under low-frequency fluctuations in resource availability, but dampened under high-frequency fluctuations (Harrison *et al.*, 2013). These different outcomes were attributed to variation in bacterial population size either increasing or decreasing the supply of favourable mutations for resistance evolution (Harrison *et al.*, 2013). Similarly, Friman *et al.* (2011a) found in a predator–prey system that low-frequency resource pulses reduced the intensity of coevolution, or induced prey biofilm formation, which predators could not overcome (Friman *et al.*, 2011b). Hiltunen *et al.* (2015) also show that temporal fluctuation in environmental stress can dampen coevolution. These are all evidence for temporal coevolutionary cold spots.

Experimental studies to date describe overall net effects of temporal environmental variation on antagonistic coevolution, but little is known about how closely coevolution can track environmental fluctuations. Can populations go back and forth between coevolutionary hot- and cold-spot states, and how is this influenced by the way environmental conditions fluctuate? To address these questions, we investigated temporal variation in abiotic stress as a coevolutionary pacemaker in a microbial host–parasite model system. We aimed to quantify how the impact of the frequency of exposure to temperature stress drives eco-evolutionary feedbacks between population dynamics and coevolution, and the occurrence of temporary coevolutionary hot and cold spots. We expected the existence of threshold phenomena where coevolution may be robust to environmental fluctuations up to a certain frequency, above (or below) which hot spots become cold spots.

We imposed temperature fluctuations on experimental microcosm populations of the bacterium *Pseudomonas fluorescens* SBW25 and the lytic phage SBWΦ2. Based on findings by Zhang & Buckling (2011), conditions were alternating between 28 °C and 32 °C, which is stressful for phage (Zhang & Buckling, 2011), every 2, 4 or 8 days, for a total period of 16 days (Fig. S1). Indeed, bacterial growth is the same at both temperatures, whereas phage cannot replicate at temperatures higher than 30 °C (Zhang & Buckling, 2011). We determined bacterial and phage densities at 2-day intervals and used standard time-shift assays (Harrison *et al.*, 2013) to compare coevolutionary rates of change in bacterial resistance and phage infectivity among fluctuation treatments. In particular, we anticipated that the slowing of coevolution would be more likely during longer periods at 32 °C in our low-frequency, temperature change treatment.

We found that regular exposure to 32 °C dampened coevolution and produced temporary coevolutionary cold spots. This effect became increasingly pronounced at lower fluctuation frequencies (4- to 8-day intervals) and thus the time spent at 32 °C. In contrast, high-frequency environmental fluctuations (2-day intervals) caused no significant deviation from the characteristic arms race dynamics (ARD)-like coevolution observed in this system at 28 °C constant (Buckling & Rainey, 2002; Brockhurst *et al.*, 2003), indicating robustness of the coevolutionary process to short pulses of stress. Correlations between temperature and phage density suggest that variation in coevolution intensity is the result of eco-evolutionary feedbacks.

Materials and methods

Biological system

We employed an isogenic strain of the bacterium *P. fluorescens* SBW25, originally isolated on sugar beet (Rainey & Travisano, 1998). The parasite is the naturally occurring lytic bacteriophage virus SBWΦ2 (Buckling & Rainey, 2002). Experimental populations were maintained in nutrient-rich King's B medium (KB), which contains 10 g glycerol L^{-1}, 20 g proteose peptone L^{-1}, 1.5 g potassium phosphate L^{-1} and 1.5 g magnesium L^{-1}. Zhang & Buckling (2011) showed that in KB medium, *P. fluorescens* growth does not differ between 28 °C and 32 °C, whereas phage growth is restricted at temperatures higher than 30 °C (Zhang & Buckling, 2011).

Experimental populations

Four days prior to the experiment (day-4), a bacterial culture was initiated by placing a previously frozen crystal of ancestral *P. fluorescens* cells in a 30-mL universal glass vial containing 6 mL of KB. On day-2, this culture was used to seed the experimental populations, by transferring ~10^7 cells to 50 new microcosms each containing 6 mL of KB.

In parallel to the above, 3 days (day-3) before the experiment, a bacterial population was started from a *P. fluorescens* crystal in 6 mL of KB. On day-2, this population was infected with phage by placing a frozen crystal of SBWΦ2 in the bacterial solution. On day-1, phage was isolated from the infected population by adding chloroform (10% chloroform: 90% microcosm population), vortexing and centrifuging for 5 min at 8000 *g*. The supernatant containing phage was used to infect ancestral bacterial populations in 30 of the experimental microcosms with ~10^5 phage particles. Twenty microcosm populations remained uninfected with phage to serve as controls. All populations were kept at 28 °C, with constant orbital agitation at 200 RPM.

Selection experiment

At the beginning of the experiment (day 0), six infected ($\log_{10}$ mean bacterial density 4.7 ± 0.15 SE) and four uninfected ($\log_{10}$ mean density 8.0 ± 0.08) bacterial microcosms were arbitrarily assigned to each of three fluctuating treatments. In these treatments, populations were moved between permissive (28 °C) and restrictive (32 °C) temperatures following (i) each transfer, every 2 days, (ii) every second transfer, every 4 days or (iii) every fourth transfer, every 8 days. Half of the populations from each fluctuating regime started the experiment at 28 °C and the other at 32 °C, thus representing treatments with the same fluctuation regime, but inverted in time (which we refer to as 'mirror treatment'). For example, the mirror treatment from the high-frequency fluctuation regime comprised three populations that spent days 1 and 2 of the experiment at 28 °C, days 3 and 4 at 32 °C, days 5 and 6 at 28 °C, days 7 and 8 at 32 °C and so on. Conversely, the three remaining populations from the high-frequency fluctuation treatment spent days 1 and 2 of the experiment at 32 °C, days 3 and 4 at 28 °C, days 5 and 6 at 32 °C and days 7 and 8 at 28 °C changing temperature every 2 days until the end of the experiment. Thus, the fluctuating treatments comprised 2 infection × 3 fluctuating × 2 mirror treatments = 12 treatments, over a total of 30 microcosms. In addition to these treatments, six infected and four uninfected bacterial microcosm populations were arbitrarily assigned to either constant 28 °C or constant 32 °C (20 microcosms in total), which served as reference treatments (see Fig. S1 for a diagram showing constant and fluctuating temperature treatments).

Experimental populations were maintained by serial transfer of 15% (900 μL) of the population to a new microcosm containing 5.1 mL of KB, every 2 days, over a 16-day period. Serial transfer of 15% of the population is higher than the 1% transferred in most other experiments with this study system [e.g. (Buckling & Rainey, 2002; Brockhurst *et al.*, 2003)]. Transfer of 15% of the population corresponds to approximately three bacterial generations per transfer. This protocol was applied to maintain phage populations at 32 °C, which would otherwise go extinct before the end of the experiment in the fluctuation treatments (see Zhang & Buckling, 2011). Microcosms were not agitated during the experiment, and vortexed only before each transfer to a new microcosm, and just after. At each transfer, phage densities were measured and a 600 μL sample of each population was added to 400 μL of glycerol and stored at −80 °C.

Bacterial densities

We measured bacterial density from the frozen samples, collected prior to each transfer every 2 days. Bacteria were serially diluted in M9 salts (128 g disodium phosphate L^{-1}, 30 g monopotassium phosphate L^{-1}, 5 g sodium chloride L^{-1} and 10 g ammonium chloride L^{-1}) and plated on to KB agar. The number of colony-forming units (CFUs) was determined after 48-h incubation at 28 °C.

Phage densities

Phage density was measured on day 0 of the experiment and then every 2 days prior to each transfer. Phages were separated from bacteria as described above and the supernatant serially diluted in M9 salts from 10^{-1} to 10^{-8}. The serially diluted phages were then spot-plated onto soft KB agar containing a lawn of ancestral bacteria. After 24-h incubation at 28 °C, phage densities were estimated by counting plaque-forming units (PFUs).

Time-shift assays

We conducted time-shift assays to measure bacteria–phage coevolution by confronting bacteria and phage from different time points. We tested for bacterial evolution by comparing the resistance of past, current and future bacteria to current phage. Conversely, we measured phage evolution by comparing the infectivity of past, current and future phage to current bacteria (as described in (Brockhurst *et al.*, 2003; Gandon *et al.*, 2008)). Time-shift assays were performed on bacteria and phage from three time periods: at the beginning, middle and end of the experiment. For each period, the time window was centred on a different contemporary combination of bacteria and phage, and went two

transfers into the past and two into the future. Thus, time-shift curves at the beginning of the experiment were centred on day 4, and the middle and end of the experiment day 8 and day 12, respectively.

Bacteria for the time-shift assays were isolated by taking 20 μL from the defrosted frozen samples, diluting in M9 salts (180 μL), plating on KB agar and incubating at 28 °C for 24 h. To extract phage, a crystal from each frozen sample was placed in 6 mL of KB and grown overnight at 28 °C, with agitation. Phage was extracted using the technique described above. Following Brockhurst *et al.* (2003), resistance and infectivity were determined by streaking up to 20 arbitrarily chosen bacterial colonies (mean 12, ±0.1 SE) across a perpendicular line of phage (20 μL) from a given microcosm population, previously placed on KB agar. A bacterial colony was defined as 'resistant' if there was no inhibition of growth, and as 'susceptible' if there was inhibition of growth. Ancestral bacteria were included in each assay as a control to ensure phages were active. All streaking tests were performed at 28 °C; it was not possible to do these tests at 32 °C, as we never observed any inhibition of bacteria growth or phage plaque formation at this temperature.

Statistical analysis

Bacterial and phage densities

We used general linear mixed models (GLMMs) to investigate how $\log_{10}$-transformed phage (+1) and bacterial densities mL^{-1} changed over the 16 days of the experiment. In different factorial models, effects of temperature treatments (constant 28 vs. 32 °C; fluctuation frequency: 2-day, 4-day, 8-day intervals) and phage presence/absence were taken as fixed factors and time as a random factor. Mirror sequence (nested within fluctuation frequency) and replicate population identity (nested within temperature treatment and mirror sequence) were included as random factors. In more detailed analyses of individual time intervals, we further analysed the effect of temperature change between transfers (28 °C → 28 °C, 28 °C → 32 °C, 32 °C → 28 °C or 32 °C → 32 °C) on the density change for both bacteria and phage. We also tested how the length of time spent at 32 °C influenced phage density.

Host and parasite coevolution

We used factorial GLMMs with a binomial error structure (logit link function) to analyse time-shift curves of bacterial resistance and phage infectivity, with the proportion of resistant bacterial colonies as the response variable (Harrison *et al.*, 2013). For bacterial evolution, models included bacterial time shift (−2, 0, +2 to denote bacteria from two transfers into the past, from the present and from two transfers into the future) as a covariate. In the same way, models for phage evolution included phage time shift as a covariate. Quadratic terms for time shift were fitted to detect deviations from linear patterns typical of arms race-like coevolution. Models included temperature treatments (28 vs. 32 °C; fluctuation frequency) and the period covered by the time shift (early, middle, late) as fixed factors, as well as mirror treatment and population identity as random nested factors.

Coevolution score

We combined evolutionary change in bacteria and in phage into a single 'coevolution score'. Arms race-like antagonistic coevolution should produce linear, crossing time-shift curves of bacteria and phage, as bacteria evolve higher resistance and phage higher infectivity through time (see Fig. 3a at 28 °C constant). Consequently, at time shift t_{+2} the bacteria curve should have higher resistance levels than the phage curve, and at time shift t_{-2} the bacteria curve should have lower resistance levels than the phage curve. We use these differences in (arcsine-transformed) resistance levels between bacteria and phage curves as a coevolution score: the higher the difference, the stronger the coevolution. Thus, the score is calculated as bacteria resistance in the bacteria time-shift curve minus bacteria resistance in the phage time-shift curve. To adjust the sign of the score, the difference between the bacteria and phage curve at t_{-2} was multiplied by −1. The coevolution score was calculated for each replicate population, time period and time shift. Furthermore, for each individual score we recorded the corresponding temperature condition (28 °C or 32 °C), to which the microcosm was exposed at the time the score was measured. We then used a GLMM to test whether this current temperature influenced the coevolution score in the different treatments. Population identity was included to account for repeated measures.

Finally, we analysed the joint action of temperature and phage or bacteria population density on coevolution. First, we performed a fully factorial multiple regression with coevolution score as response variable and current temperature and ($\log_{10}$) phage and bacteria density as covariates; replicate population was added as a random factor. Path analysis, using standardized beta-coefficients obtained from a simplified regression, was used to quantify the relative contributions of these different variables. Second, we carried out a multivariate analysis of variance with the coevolution score and phage density as response variables and temperature as an explanatory variable. If temperature was a driver of the relationship between the force of infection and coevolution, combinations of higher and lower values of coevolution score and phage density should be associated with higher and lower temperature (32 °C vs. 28 °C).

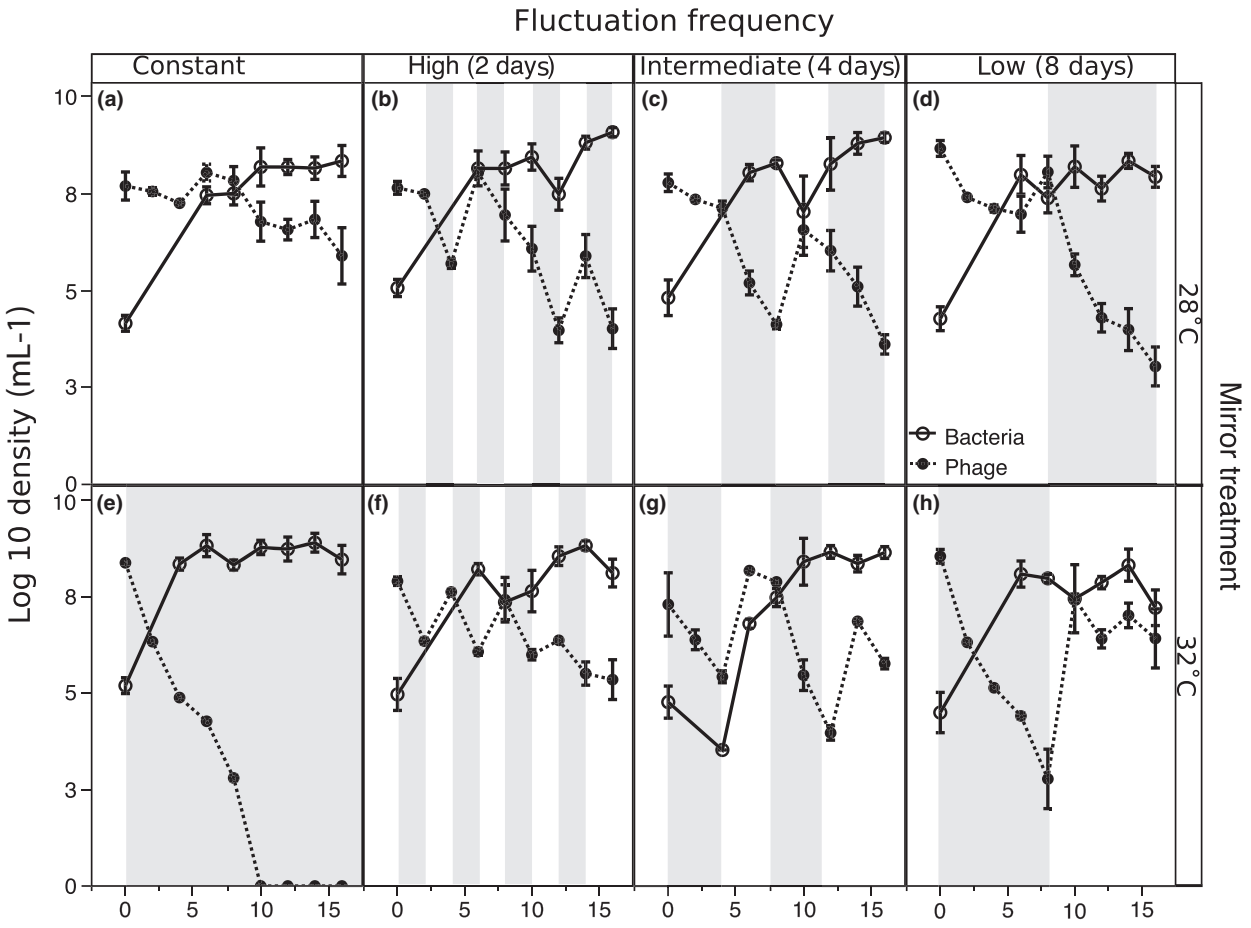

Fig. 1 Mean $\log_{10}$ bacteria (solid lines) and phage (dotted lines) density mL^{-1} in coevolving microcosm populations (±standard errors). Top panels show 'mirror treatments' starting the experiment at 28 °C and bottom panels at 32 °C. (a and e) = constant treatments, (b and f) = high fluctuation treatments (2 days), (c and g) = intermediate fluctuation treatments (4 days) and (d and h) low fluctuation treatments (8 days). A grey background indicates periods during the experiment spent at 32 °C and a white background 28 °C. [Correction added on 6 December 2016, after first online publication: Figure 1 was incorrect and has been replaced in this current version]

Where necessary, GLMMs with binomial error employed quasi F-tests to account for nested model structure and for model overdispersion (Crawley, 1993). Where appropriate, we performed backward model simplification to increase statistical power. All analyses were performed in JMP10 and 12 (SAS Institute Inc., 2012).

Results

Bacterial density

Bacterial density was not strongly affected by the different temperature treatments (Fig. 1 and Fig. S2). Overall, bacteria density was higher for infected populations at constant 32 °C than at constant 28 °C (time*temperature*phage interaction; $F_{6,93} = 2.34$, $P = 0.0376$; Fig. 1 and Fig. S2). However, there was no significant effect of fluctuation treatment on density (main effect and all interactions: $P > 0.05$), and after an initial increase during the first week of the experiment, densities remained fairly constant in all treatments. We further detected no significant relationship between the temperature experienced between transfers and bacterial density changes ($F_{3,96} = 1.6854$, $P = 0.1753$). In contrast, as expected, bacterial densities were significantly reduced by phage throughout the entire experiment (constant temperature: $F_{1,8} = 12.10$, $P = 0.0082$; variable temperature: $F_{1,29} = 24.03$, $P = 0.0010$; Fig. S2).

Phage density

Phage densities remained more or less unchanged at constant 28 °C, but declined rapidly at 32 °C, with extinction observed in all populations by day 10 (Fig. 1). In the different variable temperature treatments, phage densities fluctuated over time (mirror

treatment*time[fluctuation frequency]: $F_{24,91} = 21.55$, $P = 0.0217$; Fig. 1). Additional analyses showed that phage density tracked changes in temperature declining when changed to, or remaining at, 32 °C and increasing when changed from 32 °C to 28 °C (Figs 1 and 2) (direction of temperature change: $F_{3,66} = 61.16$, $P < 0.0001$). Prolonged exposure to 32 °C was associated with a stronger decline in phage density ($F_{1,96} = 410$, $P < 0.0001$; Fig. 1 and Fig. S3). However, none of the phage populations went extinct in the fluctuating treatments, even during 8 days of 32 °C at the lowest fluctuation frequency.

Time-shift analyses: bacteria and phage (co) evolution

Constant temperature

At constant 28 °C, time-shift analysis revealed significant linear increases in bacterial resistance (time shift: $\chi^2_1 = 13.02$, $P = 0.0003$) and in phage infectivity (time shift: $\chi^2_1 = 5.25$, $P = 0.0220$), producing crossing time-shift curves indicative of ARD-like coevolution (Fig. 3a). There was no significant nonlinearity of time-shift curves (time shift^2 and interactions: $P > 0.3982$). Further, there was a significant effect of time period ($\chi^2_2 = 8.00$, $P = 0.0183$), showing that bacteria were becoming increasingly resistant to their coevolving phage over the course of the experiment. This was mirrored by the opposite trend of decreasing phage infectivity through time ($\chi^2_2 = 8.41$, $P = 0.0149$). In contrast, at constant 32 °C, there was no evidence for resistance evolution. Phages remained capable of infecting > 95% of their bacteria, before going extinct between days 8 and 10 (Fig. 3e).

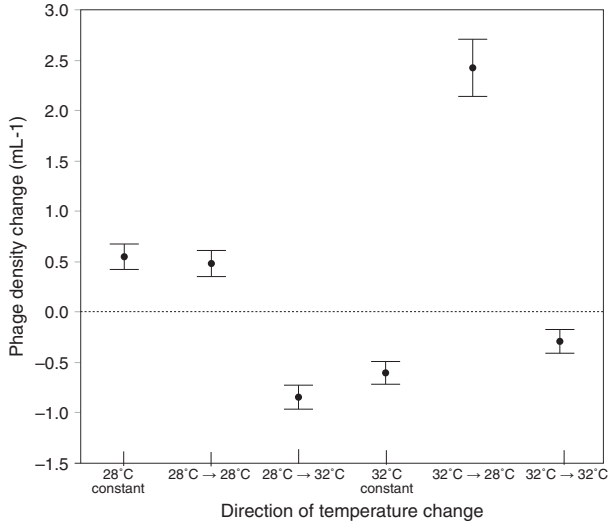

Fig. 2 Mean change in phage density (measured using PFU) in constant 28 °C and 32 °C treatments and in the fluctuating temperature treatments when populations remain at the same temperature (28 → 28, 32 → 32) or following a temperature change (32 → 28 or 28 → 32) between transfers (±standard error). Dashed line corresponds to no change in phage density.

Variable temperature

Fluctuating treatments showed considerable deviations from the regular linear patterns observed at constant 28 °C. For bacterial evolution, we found evidence for nonlinear changes in resistance (time-shift^2: $\chi^2_1 = 22.25$, $P < 0.0001$). Moreover these nonlinear effects varied significantly with fluctuation treatment and reference time period (time-shift^2*fluctuation frequency*time period: $\chi^2_4 = 16.64$, $P = 0.0023$; Fig. 3). Some of this variation is explained by relatively flat parts of time-shift curves when at 32 °C (Fig. 3), meaning no resistance evolution during exposure to high temperature. This effect was particularly evident in the lowest fluctuation treatment, with 8 days of exposure to 32 °C (Fig. 3d).

Patterns of phage evolution were mostly linear (time-shift: $\chi^2_1 = 8.71$, $P = 0.0032$) and showed no significant deviation from nonlinearity (all time-shift^2 terms: $P > 0.6894$). Nonetheless, time-shift curves differed between mirror sequences of the same fluctuation treatments (mirror sequence*time-shift [fluctuation frequency]: $\chi^2_3 = 10.63$, $P = 0.0139$), indicating at least some degree of temperature-dependent evolution. Overall, Fig. 3 shows more regular coevolution for 2- and 4-day temperature fluctuation treatments (crossing time-shift curves in four of six panels, respectively) than for the 8-day fluctuation treatment (crossing in one of six panels). Formal analysis of these patterns is presented below.

Analysis of the 'coevolution score'

At constant 28 °C, we observed a significant positive coevolution score ($t_{32} = 4.1$, $P = 0.0003$, Fig. 4), consistent with the crossing time-shift curves in Fig. 3a and the occurrence of ARD-like coevolution. In contrast, no significant sign of coevolution was detected at constant 32 °C ($t_{11} = 1.81$, $P = 0.0962$, Fig. 4). The coevolution score enabled us to distil consistent temperature effects across fluctuating treatments that were less clear from time-shift curves. Namely, a significant temperature by fluctuation frequency interaction shows that the effect of fluctuation frequency on the coevolution score depended on the current temperature at which the score was measured (current temperature*fluctuation frequency: $F_{2,80} = 3.65$, $P = 0.0305$, Fig. 4). Under high-frequency fluctuations, current temperature did not significantly impact the coevolution score, whereas under lower-frequency fluctuations (4- and 8-day), coevolution scores at 32 °C were lower than those at 28 °C. Scores were always positive at 28 °C, but declined with increasing

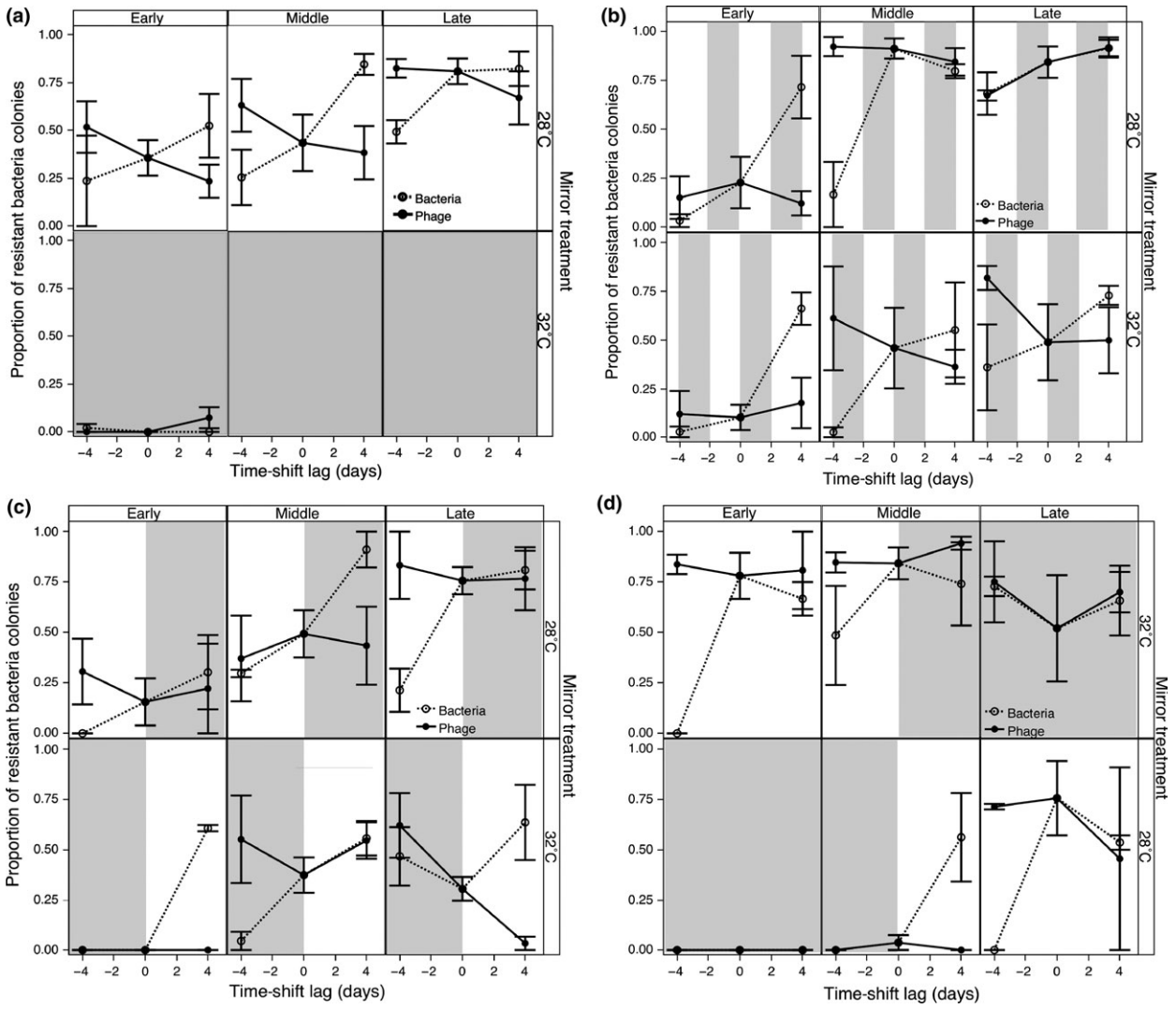

Fig. 3 Time-shift curves measuring coevolution as change in bacteria resistance (dashed lines) and phage infectivity (solid lines) as the proportion of bacteria resistant to phage. Bacteria (phage) time-shifts show mean bacteria (phage) resistance of past, contemporary and future bacteria when confronted with contemporary phage (bacteria) at the beginning, middle and end of the experiment (+standard error). Panel a) = constant environments, b) = high-frequency fluctuations, c) = intermediate-frequency fluctuations and d) = low-frequency fluctuations. Grey blocks represent periods of time at 32 °C.

exposure to 32 °C, with complete inhibition of coevolution at the lowest fluctuation frequency after 8 days at 32 °C.

Overall, 32 °C was associated with lower phage density and coevolution score, whereas 28 °C was associated with higher density and score (Fig. 5, showing the relationship across treatment means). Multiple regression did not find an effect of bacterial density on the coevolution score (all $P > 0.12$). However, phage density had a significant positive effect on the score when fitted first ($F_{1,125} = 8.40$, $P = 0.0044$), but became nonsignificant ($F_{1,133} = 2.62$, $P = 0.1077$) once temperature was included in the model ($F_{1,138} = 9.86$, $P = 0.0021$). Path analysis summarizes the relationships between these different variables (Fig. 6) showing a significant, independent effect of current temperature on coevolution score, but also partial confounding of current temperature and phage density (why phage density is nonsignificant when both factors are fitted in the multiple regression model). Results from an additional multivariate analysis of variance corroborate an indirect action of current temperature via phage density, as shown by the significant effect of temperature on the association between coevolution score and phage density ($F_{1,138} = 9.86$, $P = 0.0021$).

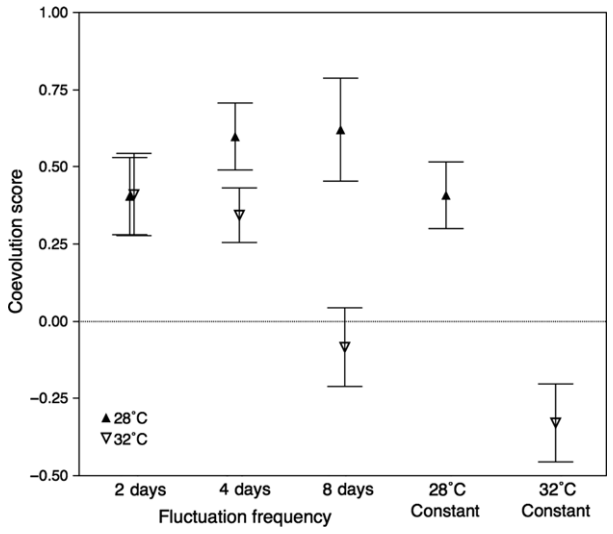

Fig. 4 Mean coevolution score (±standard error), measured as difference in bacterial resistance between bacteria and phage time-shift curves at time-shift ± 4 at constant 28 °C and 32 °C, and in the different fluctuation treatments during periods when populations were at 28 °C (closed triangles) and 32 °C (open triangles). The solid line crossing zero represents no arms race dynamics coevolution.

Discussion

Our imposed temperature fluctuations, alternating between 28 °C and 32 °C, induced temporary coevolutionary hot and cold spots between *P. fluorescens* SBW25 and its phage Φ2. Coevolutionary cold spots occurred during prolonged exposure (4 and 8 days) to 32 °C under intermediate and low frequencies of temperature change. Nevertheless, coevolution resumed once populations were returned to permissive temperatures of 28 °C and was only completely absent from populations experiencing 32 °C constant. In contrast, under high-frequency fluctuations (2-day intervals of exposure to 32 °C), the strength of coevolution was similar to that observed in the 28 °C constant treatment. Indeed, 28 °C constant produced a coevolutionary hot spot, characterized by arms race-like dynamics with monotonic increases in resistance and infectivity, as is often found for this system (e.g. (Brockhurst *et al.*, 2003; Lopez-Pascua & Buckling, 2008; Morgan *et al.*, 2010)).

Temporary coevolutionary hot and cold spots

Contrary to our experiment, Harrison *et al.* (2013) showed, in the same system, that high-frequency fluctuations in resource availability prevented coevolution, whereas low-frequency fluctuations had no effect. They explain this effect by lower resource conditions leading to lower bacterial density and thus fewer favourable mutants, impeding selective sweeps in bacterial resistance (Harrison *et al.*, 2013). Unlike in Harrison *et al.*'s study (2013; see also Friman & Laakso, 2011a; Friman *et al.*, 2011b), our temperature treatments affected phage rather than bacterial densities. Hiltunen *et al.* (2015) found that coevolution was most slowed under simultaneous application of two different stressors: one affecting predators and the other affecting prey. Furthermore, we did not only look at the overall net effect of temporal environmental variation on coevolution, but also at what occurs at shorter timescales by analysing temporary changes in the coevolution score during periods of 28 °C or 32 °C. This revealed a negative linear relationship between the time spent at 32 °C and the coevolution score, with a minimum threshold amount of time (~4 days) needed to induce a temporary coevolutionary cold spot. The absence of a temperature signal for the 2-day fluctuation treatment indicates that 2 days at 32 °C were insufficient to stall the coevolutionary process. Conversely, there was no corresponding effect of the time spent at 28 °C, suggesting that even short periods of permissive temperature immediately generate a coevolutionary hot spot.

Eco-evolutionary feedbacks

The importance of tight links between demography and coevolution, 'eco-evolutionary feedbacks', driving host–parasite dynamics (densities and resistance and infectivity evolution) is only beginning to be understood (Bohannan & Lenski, 2000; Bull *et al.*, 2006; Hiltunen & Becks, 2014; Penczykowski *et al.*, 2015). Here, we provide a detailed quantitative investigation of such a link. Across treatments and temperatures, we observed a positive relationship between phage density and the coevolution score (Fig. 5). Furthermore, phage densities closely tracked temperature changes, increasing and decreasing during periods of 28 °C and 32 °C, respectively (Fig. 1). Consequently, higher phage density and coevolution were observed at 28 °C, and lower phage density and coevolution at 32 °C. These patterns suggest a temperature-mediated eco-evolutionary feedback, whereby lower phage density at 32 °C lowers phage–bacteria encounter rates (i.e. the force of infection) and, consequently, reduces the intensity of coevolution. At the same time, smaller phage populations may lack a supply of favourable mutations for simultaneous coevolution with bacteria and adaptation to 32 °C. A possible explanation for the observed decline in phage density is that higher temperature damages or inactivates phage (De Paepe & Taddei, 2006). This is in line with results from an additional experiment, showing that phage titres in the external environment decline at higher rates at 32 °C than 28 °C (Fig. S4). It also fits with our observation of phage extinction after 10 days at 32 °C constant.

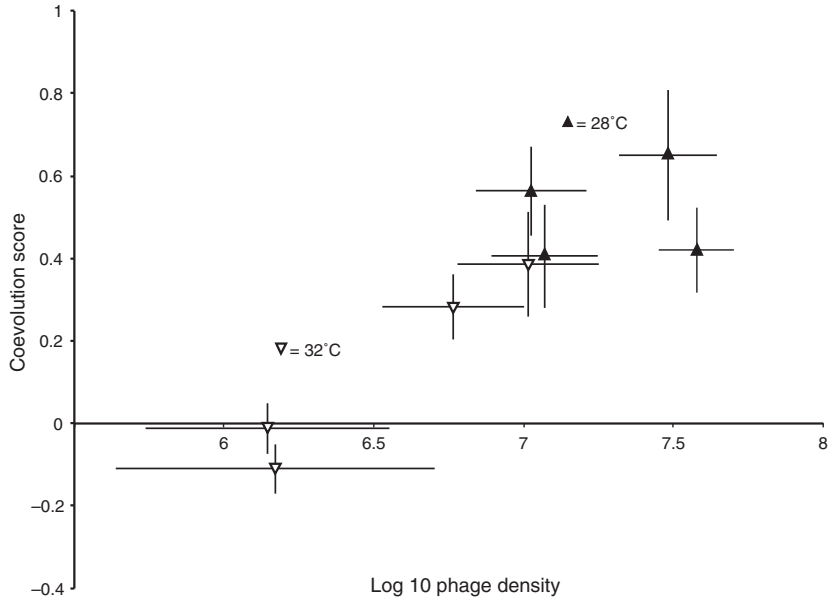

Fig. 5 Mean coevolution score (±standard error) as a function of mean phage density (±standard error) over all treatment combinations for constant and fluctuating temperature environments when at 28 °C (black triangles) and 32 °C (white triangles) (±standard error).

Interestingly, more detailed analysis showed that the temperature effect cannot be fully accounted for by its (indirect) action on phage density. We speculate that an additional temperature effect is caused by changes in bacteria. High temperature may lead to modified expression of bacterial surface proteins, preventing phage adhesion to cell walls (Sillankorva *et al.*, 2004). Such modifications would reduce the density of susceptible bacteria available for infection, yet remain undetected in analyses, because our density measurements do not discriminate between susceptible and resistant cells. This illustrates the limitations of using correlative analyses to uncover eco-evolutionary feedbacks. Here, only temperature was manipulated experimentally. More rigorous tests of the role of the force of infection would require the manipulation of bacterial or phage density, or both (Turner *et al.*, 1998).

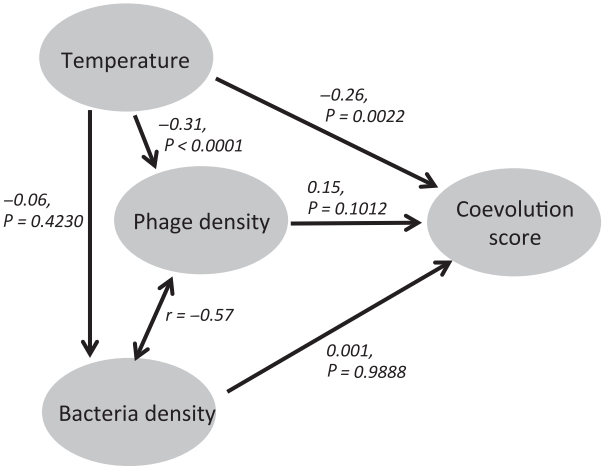

Fig. 6 Path analysis disentangling the direct and indirect effects of temperature, log 10 phage and bacteria density on the coevolution score. Numbers beside one-way arrows denote path correlation coefficients calculated using standardized beta-regression coefficients with *P*-values from associated regression analyses. The relationship between $\log_{10}$ bacteria and phage density remains unanalysed, as directionality is unknown (the number beside the two-way arrow is the correlation coefficient).

Broader implications

Partial overlap of ecological niches may generate variation in the strength and intensity of coevolution between natural enemies over their geographic range (Thompson, 2005). Thus, situations may exist, where conditions within a species range are ecological sinks for exploiters, but not victims (Kirkpatrick & Barton, 1997; Nuismer & Gandon, 2008). This may generate coevolutionary cold spots in such areas and provide spatial refuges for victims. We show that the same idea also applies to temporally variable environments. One main difference with a spatial scenario is that the same population can experience coevolutionary temporary cold and hot spots over time (Nuismer *et al.*, 2003). Indeed, in our case, all populations experienced change in both directions, but importantly, there was a memory effect. Evolved resistance was not lost during periods at 32 °C, suggesting there were negligible costs of coevolutionary cold spots in terms of reduced resistance when coevolution resumes. Hence, periods of stress for the exploiter may create a temporary refuge for the victim, without compromising its coevolutionary potential.

We find that coevolution is resilient to environmental disturbance, as it always resumed even after eight consecutive days at 32 °C in the low-frequency treatments. However, we also found that just two additional days at 32 °C were enough to invariably cause phage extinction. We postulate that low-frequency fluctuations with prolonged exposure to stress create unstable states, where there is potential for a coevolutionary hot spot to either re-establish, or to irreversibly become a cold spot. In our populations, phage density appears to be the crucial parameter defining such a 'tipping point'. The density of active phage decreased linearly with time at 32 °C. Thus, epidemiological fade-out and phage extinction may become increasingly probable when phage density falls below critical levels. Our results suggest that system instability covers a relatively small parameter space (here: 1–2 orders of magnitude in phage density) and/or a short time window (≈3 host generations), before collapse occurs invariably.

Conclusions

Our new metric for coevolution, the 'coevolution score', shows that environmental fluctuations in temperature induced temporary coevolutionary hot and cold spots that can be turned on and off repeatedly, without extinction of either antagonist. Accordingly, coevolution in terms of infectivity and resistance traits may occur on different temporal states and at different spatial locations in spatially heterogeneous systems (Thompson, 2005). Future studies should extend theoretical models of spatiotemporal antagonistic coevolution (Gandon *et al.*, 1996; Hochberg & van Baalen, 1998) to incorporate extreme environments for either or both antagonist.

Our study further provides a quantitative analysis of eco-epidemiological feedbacks. It suggests that temporary high temperature caused declines in susceptible host density, thereby reducing encounter rates, leading to a coevolutionary cold spot. Importantly, we show that cold spots may be threshold-dependent, arising only for environmental fluctuations with sufficiently long exposure to adverse conditions.

Finally, our results question the notion that climate change induced increases in mean temperatures will exacerbate parasite spread and severity (Altizer *et al.*, 2013). Rather, a change in the mean is likely accompanied by a change in the frequency of exposure to extreme conditions, which may be key to setting coevolutionary speed limits or obstructing parasite persistence altogether. Indeed, knowledge of the amplitude and frequency distribution of extreme conditions is likely to be essential for predictions in epidemiology and coevolution (Paaijmans *et al.*, 2010; Duncan *et al.*, 2011; Heilmann *et al.*, 2012). However, as highlighted by Altizer *et al.* (2013), the impact of extreme conditions will depend on the details of the underlying biology of host–parasite interactions, and as we have shown, the extent to which a parasite's niche overlaps with that of its host.

Acknowledgments

This work was supported by grants from the James S. McDonnell Foundation Studying Complex Systems Research Award 220020294 (to M.E.H.), the Agence National de la Recherche 'EvolStress' ANR-09-BLAN-099-01 (to M.E.H. and O.K.) and the German Research Foundation (priority programme Host-Parasite Coevolution BE-2299/5-1; RA-1920/1-1 to E.D.). This is ISEM contribution ISEM 2016-201.

References

Altizer, S., Ostfeld, R.S., Johnson, P.T.J., Kutz, S. & Harvell, C.D. 2013. Climate change and infectious diseases: from evidence to a predictive framework. *Science* **341**: 514–519.

Bohannan, B.J.M. & Lenski, R.E. 2000. Linking genetic change to community evolution: insights from studies of bacteria and bacteriophage. *Ecol. Lett.* **3**: 362–377.

Brockhurst, M.A., Morgan, A.D., Rainey, P.B. & Buckling, A. 2003. Population mixing accelerates coevolution. *Ecol. Lett.* **6**: 975–979.

Buckling, A. & Rainey, P.B. 2002. Antagonistic coevolution between a bacterium and a bacteriophage. *Proc. Biol. Sci.* **269**: 931–936.

Bull, J.J., Millstein, J., Orcutt, J. & Wichman, H.A. 2006. Evolutionary feedback mediated through population density, illustrated with viruses in chemostats. *Am. Nat.* **167**: E39–E51.

Crawley, M.J. 1993. *GLIM for Ecologists*. Blackwell Science, Oxford.

De Paepe, M. & Taddei, F. 2006. Viruses' life history: towards a mechanistic basis of a trade-off between survival and reproduction among phages. *PLoS Biol.* **4**: e193.

Duncan, A.B., Fellous, S. & Kaltz, O. 2011. Temporal variation in temperature determines disease spread and maintenance in Paramecium microcosm populations. *Proc. Biol. Sci.* **278**: 3412–3420.

Forde, S.E., Thompson, J.N. & Bohannan, B.J.M. 2004. Adaptation varies through space and time in a coevolving host-parasitoid interaction. *Nature* **431**: 841–844.

Friman, V.-P. & Buckling, A. 2013. Effects of predation on real-time host-parasite coevolutionary dynamics. *Ecol. Lett.* **16**: 39–46.

Friman, V.-P. & Laakso, J. 2011a. Pulsed-resource dynamics constrain the evolution of predator-prey interactions. *Am. Nat.* **177**: 334–345.

Friman, V.-P., Laakso, J., Koivu-Orava, M. & Hiltunen, T. 2011b. Pulsed-resource dynamics increase the asymmetry of antagonistic coevolution between a predatory protist and a prey bacterium. *J. Evol. Biol.* **24**: 2563–2573.

Gandon, S., Capowiez, Y., Dubois, Y., Michalakis, Y. & Olivieri, I. 1996. Local adaptation and gene-for-gene coevolution in a metapopulation model. *Proc. R. Soc. Lond. B* **263**: 1003–1009.

Gandon, S., Buckling, A., Decaestecker, E. & Day, T. 2008. Host-parasite coevolution and patterns of adaptation across time and space. *J. Evol. Biol.* **21**: 1861–1866.

Gibert, J.P., Pires, M.M., Thompson, J.N. & Guimarães, P.R. 2013. The spatial structure of antagonistic species affects coevolution in predictable ways. *Am. Nat.* **182**: 578–591.
Gómez, P. & Buckling, A. 2011. Bacteria-phage antagonistic coevolution in soil. *Science* **332**: 106–109.
Gomulkiewicz, R., Thompson, J., Holt, R., Nuismer, S. & Hochberg, M. 2000. Hot spots, cold spots, and the geographic mosaic theory of coevolution. *Am. Nat.* **156**: 156–174.
Gorter, F.A., Scanlan, P.D. & Buckling, A. 2016. Adaptation to abiotic conditions drives local adaptation in bacteria and viruses coevolving in heterogeneous environments. *Biol. Lett.* **12**: 20150879.
Harrison, E., Laine, A.-L., Hietala, M. & Brockhurst, M.A. 2013. Rapidly fluctuating environments constrain coevolutionary arms races by impeding selective sweeps. *Proc. Biol. Sci.* **280**: 20130937.
Heilmann, S., Sneppen, K. & Krishna, S. 2012. Coexistence of phage and bacteria on the boundary of self-organized refuges. *Proc. Natl. Acad. Sci. USA* **109**: 12828–12833.
Hiltunen, T. & Becks, L. 2014. Consumer co-evolution as an important component of the eco-evolutionary feedback. *Nat. Commun.* **5**: 5226.
Hiltunen, T., Ayan, G., Becks, L., Ayan, B. & Becks, L. 2015. Environmental fluctuations restrict eco-evolutionary dynamics in predator – prey system. *Proc. R. Soc. Lond. B* **282**: 20150013.
Hochberg, M.E. & van Baalen, M. 1998. Antagonistic coevolution over productivity gradients. *Am. Nat.* **152**: 620–634.
Kirkpatrick, M. & Barton, N.H. 1997. Evolution of a species' range. *Am. Nat.* **150**: 1–23.
Lopez-Pascua, L.D.C. & Buckling, A. 2008. Increasing productivity accelerates host-parasite coevolution. *J. Evol. Biol.* **21**: 853–860.
Lopez-Pascua, L.D.C., Brockhurst, M.A. & Buckling, A. 2010. Antagonistic coevolution across productivity gradients: an experimental test of the effects of dispersal. *J. Evol. Biol.* **23**: 207–211.
Morgan, A.D., Bonsall, M.B. & Buckling, A. 2010. Impact of bacterial mutation rate on coevolutionary dynamics between bacteria and phages. *Evolution* **64**: 2980–2987.
Mostowy, R. & Engelstädter, J. 2011. The impact of environmental change on host-parasite coevolutionary dynamics. *Proc. R. Soc. Lond. B* **278**: 2283–2292.
Nuismer, S.L. & Gandon, S. 2008. Moving beyond common-garden and transplant designs: insight into the causes of local adaptation in species interactions. *Am. Nat.* **171**: 658–668.
Nuismer, S.L., Gomulkiewicz, R. & Morgan, M.T. 2003. Coevolution in temporally variable environments. *Am. Nat.* **162**: 195–204.
Paaijmans, K.P., Blanford, S., Bell, A.S., Blanford, J.I., Read, A.F. & Thomas, M.B. 2010. Influence of climate on malaria transmission depends on daily temperature variation. *Proc. Natl. Acad. Sci. USA* **107**: 15135–15139.
Penczykowski, R.M., Laine, A.-L. & Koskella, B. 2015. Understanding the ecology and evolution of host-parasite interactions across scales. *Evol. Appl.* **9**: 37–52.
Poisot, T., Thrall, P.H. & Hochberg, M.E. 2011. Trophic network structure emerges through antagonistic coevolution in temporally varying environments. *Proc. R. Soc. Lond. B* **279**: 299–308.
Rainey, P.B. & Travisano, M. 1998. Adaptive radiation in a heterogeneous environment. *Nature* **32**: 69–72.
SAS Institute Inc. 2012. *Jmp In, Version 10.1*. SAS Institute Inc., Cary, NC.
Sillankorva, S., Oliveira, R., Vieira, M.J., Sutherland, I. & Azeredo, J. 2004. *Pseudomonas fluorescens* infection by bacteriophage Φs1: the influence of temperature, host growth phase and media. *FEMS Microbiol. Lett.* **241**: 13–20.
Thompson, J.N. 2005. *The Geographic Mosaic of Coevolution*. The University of Chicago Press, Chicago.
Thompson, J.N. 2009. The coevolving web of life. *Am. Nat.* **173**: 125–140.
Thrall, P.H., Hochberg, M.E., Burdon, J.J. & Bever, J.D. 2007. Coevolution of symbiotic mutualists and parasites in a community context. *Trends Ecol. Evol.* **22**: 120–126.
Turner, P.E., Vaughn, S.C. & Lenski, R.E. 1998. Tradeoff between horizontal and vertical modes of transmission in bacterial plasmids. *Evolution* **52**: 315–329.
Vogwill, T., Fenton, A., Buckling, A., Hochberg, M.E. & Brockhurst, M.A. 2009. Source populations act as coevolutionary pacemakers in experimental selection mosaics containing hotspots and coldspots. *Am. Nat.* **173**: E171–E176.
Wolinska, J. & King, K.C. 2009. Environment can alter selection in host-parasite interactions. *Trends Parasitol.* **25**: 236–244.
Zhang, Q.-G. & Buckling, A. 2011. Antagonistic coevolution limits population persistence of a virus in a thermally deteriorating environment. *Ecol. Lett.* **14**: 282–288.

Supporting information

Additional Supporting Information may be found online in the supporting information tab for this article:
Figure S1 The diagram shows the different temperature treatments for microcosm populations of *Pseudomonas fluorescens* infected with the lytic phage SBWΦ2.
Figure S2 Mean $\log_{10}$ bacteria density mL^{-1} in infected (solid lines, open circles) and uninfected (dotted lines, closed circles) in coevolving microcosm populations (±standard errors).
Figure S3 Decline in $\log_{10} + 1$ phage density mL^{-1} as a function of time in constant populations (open triangles, dashed line) and variable treatment (2 day fluctuations = open circles, 4 days = filled squares and 8 days = filled diamonds) populations.
Figure S4 Phage decline after 24 and 48 h at 28 °C (closed circles) and 32 °C (open circles).

Data deposited at Dryad: doi: 10.5061/dryad.vv29r

Received 4 August 2016; revised 26 September 2016; accepted 2 October 2016